ELSEVIER

Powder Technology 119 (2001) 81–88

POWDER TECHNOLOGY

www.elsevier.com/locate/powtec

Description of multi-particle systems using Voronoi polyhedra

Y.C. Liao [a], D.J. Lee [a,b,*], Bing-Hung Chen [b]

[a] *Department of Chemical Engineering, National Taiwan University, Taipei 10617, Taiwan*
[b] *Department of Chemical Engineering, National University of Singapore, Singapore 119260, Singapore*

Received 17 August 1999; received in revised form 7 July 2000; accepted 23 August 2000

Abstract

This study performed Voronoi polyhedra (VP) analysis to describe simulated multi-particle systems with controlled disorderliness. The methodology employed herein initiates with a fixed number of particles (ranging from 64 to 256) on various lattice sites (fcc, bcc and sc). The position of each particle is then perturbed using three different methods, with the magnitude being controlled by the variable p. Voronoi analysis is then conducted for various p, and the probability distributions of the number of faces, area, volume, and asphericity factor are then calculated. Also discussed herein is the ability of these VP characteristics to detect the solid/liquid and liquid/gas transitions.

Keywords: Voronoi polyhedra; Disorderliness; RDF

1. Introduction

Voronoi polyhedra (VP) are defined as the convex region of the close space to their own central particle, which tessellate and fill the space of the multi-particle system [1]. The Voronoi–Delaunay tessellation, which was introduced to analyze random close packing of hard spheres [2–5], has been applied in identifying microstructures of Lennard–Jones (LJ) materials or amorphous solids [6–13]. Previous studies [14,15] summarize the applications for calculating volume occupied by atoms. Other applications include the perspective of determining crystal structures [16,17], material science [18,19], biology [20,21], hollow-fiber contractors [22], packing of fixed-beds [23], and others.

The VP analysis is particularly effective for examining the local structure of multi-particle systems. The distributions of volume, surface area, numbers of faces and asphericity parameter (η) of VP occupied by constituting particles describe microstructures better than the radial distribution function (RDF), since the latter averages out the structural information along the radial direction. Ruocco et al. [7] employed the asphericity parameter to differentiate the structural change in an ice crystal with decreasing temperature. The η value is defined as $A^3/36\pi V^2$, where A and V are the surface area and volume of VP, respectively. η denotes unity for a sphere and is greater than unity for the other shapes (for example, body-centered cubic, 1.33; octahedron, 1.65; simple cubic, 1.91; and tetrahedron, 3.31). Shih et al. [11] also employed η to identify the local structure of liquid water. Furthermore, Montoro and Abascal [9] investigated the structures of LJ materials based on anisotropic factors. These authors all suggested that η is superior to the other VP characteristics in differentiating the detailed structures among phases. Everett [24] estimated the configurational entropy changes according to the face distribution of VP. Meanwhile, Hsu and Mou [8] employed this approach to estimate the entropy change during the melting of an LJ solid. Liao and Lee [25] investigated the feasibility of using VP to detect the existence of channels in the multi-particle systems.

Previous simulation works considered the interactions between particles. According to the total interaction energy level, only certain configurations are reasonably likely to be achieved, for example, stable gas or stable liquid states. The judgment that the VP descriptors are superior is generally based upon some a priori knowledge of the system's physical state. For example, Montoro and Abas-

* Corresponding author. Department of Chemical Engineering, National Taiwan University, Taipei 10617, Taiwan. Tel.: +886-2-2363-5230; fax: +886-2-2362-3040.

E-mail address: djlee@ccms.ntu.edu.tw (D.J. Lee).

0032-5910/01/$ - see front matter
PII: S0032-5910(00)00408-3

cal [9] noted that the anisotropic factors differentiated the liquid and the quenched solid states in specific systems better than the volume and face distribution could, and thus concluded that the former is a better microstructural descriptor than the latter two. The general ability of VP to describe the configurations of a multi-particle system remains unclear. Notably, VP consider only the system configurations and neglect the energy levels of the system. This study employs VP to describe a multi-particle system with a controlled disorderliness. The various VP indices proposed previously are compared herein based on their ability to detect configurational changes at controlled perturbations.

2. Methods

A total of $4 \times 4 \times 4$ unit cells allocated in a cube of unit length are considered herein. The unit cells could be face-centered cubic (fcc) lattice, body-centered cubic (bcc) lattice or a simple cubic (sc) lattice. The number of particles is thus 256 for fcc, 128 for bcc and 64 for sc, respectively. (The term "particle" here denotes a point occupying no volume and having no interactions with the other "particles" in the system.) Periodical boundary conditions were applied to simulate an infinite system. Fig. 1 displays the cube and the three lattices investigated herein.

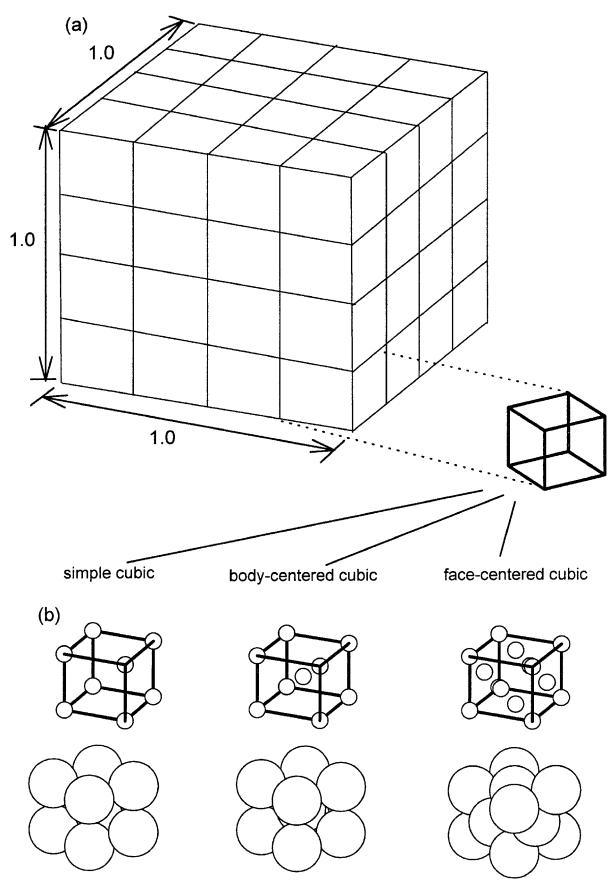

Fig. 1. (a) The cube of unit length, (b) the three lattices under investigation.

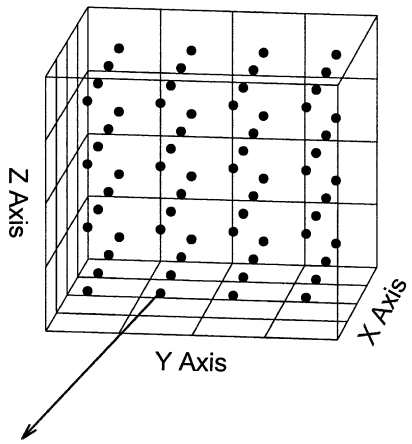

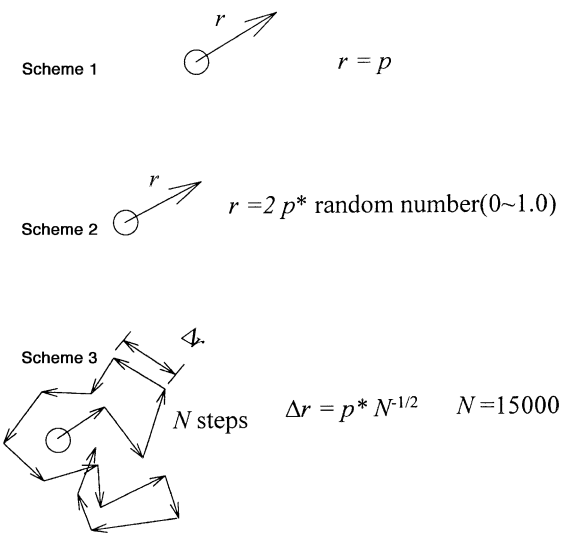

Fig. 2. The three schemes employed to perturb the lattice.

To construct a multi-particle system with a controlled disorderliness, the positions of each particle were perturbed in one of the following three schemes (Fig. 2). The spherical coordinates for every particle comprise three variables: radius and two angular variables. Scheme 1 perturbs every particle from its original position by a fixed radial distance p, with the two angular variables being randomly chosen. Scheme 2 resembles Scheme 1 except that the perturbed radial distance is a random variable whose probability is a uniform distribution at a mean of p. Meanwhile, Scheme 3 adopted a random walk scheme, which allowed the particle to randomly move N steps from its original position. The length of each step is Δr where $\Delta r = p * N^{-1/2}$. Consequently, the probability distribution of particle radial displacement is nearly a Gaussian distribution with a mean of p. (Note: N is taken as 15,000 herein, the value which is found sufficient to generate a

Gaussian distribution independent of N.) According to the three schemes mentioned above, a multi-particle system can be generated in which disorderliness is controlled by the parameter p, with higher p denoting a more disorderly system. Inasmuch as the present schemes overlook the energy constraint, the effects of changing system disorderliness on the VP constructions can be studied continuously.

The Voronoi analysis was conducted by the method proposed by Tanemura et al. [26], from which the normalized probability distributions of the number of faces, area (A), volume (V) and asphericity parameter (η) of VP were calculated. All distributions are ensemble averages over 100 independent configurations. Furthermore, the p value for different lattices was reported on the unit of the corresponding unit cells. For example, $p = 0.2$ denotes a perturbed distance of 20% of the unit cell (not the cube length).

The concept of configurational entropy had been proposed to identify where/when the phase changes occur [8,24]. The Boltzmann–Gibbs entropy (S) of a continuous property is defined as follows:

$$S = \int \Psi(b)\ln\Psi(b)\,\mathrm{d}b, \tag{1}$$

where Ψ presents the probability density function of the physical quantity b. (The reference for b is set at 1.0.) The discrete form of the integrand can be approximated as follows:

$$S \cong -\sum_{0}^{\infty} \frac{f_i}{\Delta b}\ln\left(\frac{f_i}{\Delta b}\right)\Delta b = \ln(\Delta b) - \sum_{0}^{\infty} f_i \ln f_i, \tag{2}$$

where $\Psi = f_i/\Delta b$. Consequently, the entropy of a distribution of b is defined herein as:

$$S_b = -\int_0^{\infty} \Psi(b)\ln(\Psi(b))\,\mathrm{d}b - \ln(\Delta b) \cong -\sum_{0}^{\infty} f_i \ln f_i, \tag{3}$$

which resembles the Kullback–Leiber entropy.

3. Results and discussion

Fig. 3 displays the RDFs for a bcc lattice subject to Scheme 1 at various magnitudes p. The RDFs obtained for the simulated systems from the other two schemes are close, indicating that the present result can cover a wide range of interest. In sum, at $p = 0.01$, the simulated system displays crystal-like characteristics. Around $p =$ 0.1–0.2, a transition occurs where the RDF transforms from being crystal-like to liquid-like. When $p = 0.3$–0.6, the RDF changes from being liquid-like to gas-like. When p exceeds 0.8, the RDF becomes flat, denoting a completely random distribution (ideal gas) [9]. For convenience, the terms "solid", "liquid" and "gas" are used herein to represent the configurations whose RDF resembles a solid, liquid, and gas, respectively.

Fig. 4 illustrates the volume distributions for bcc lattice. The total volume of the system is fixed, and consequently the normalized mean is unity. Meanwhile, Fig. 5 illustrates the corresponding variances and the M_3 value of the distributions. M_3 is defined as (the third moment of distribution)/(variance)$^{1.5}$ [14]. A distribution with a positive M_3 skews rightwards. (Note: Since the particles are randomly perturbed, Fig. 5 contains fluctuations.) When $p <$ 0.1, the configuration exhibits a single-peak characteristic that corresponds to the crystal structure. The corresponding variance and M_3 are essentially zero in this situation. As p increases above 0.1, the distribution broadens, as illustrated in Fig. 4, whose variance increases accordingly. A positive M_3 value indicates that the system includes rather large VP cells. As p exceeds 0.6, the volume distribution broadens further, but does so more slowly. At a p of over 2.0, the distribution becomes independent of p. The gas-like RDF corresponds to the distributions displayed in Fig. 4 for $p > 0.8$. Notably, the change in variance of the volume distribution of VP is less sensitive to the solid/liquid transition than the variance for RDFs. However, the volume distribution does reflect the detailed information involving configurations between liquid and gas states, which is not achievable by RDFs.

With a very large p, both variance and M_3 values level off, as they reach the ideal gas state. Notably, the plateau value for sc is less than for the other two lattices. Fig. 6 presents the cases with three sc lattices: $4 \times 4 \times 4$, $6 \times 6 \times 6$ and $10 \times 10 \times 10$ unit cells, demonstrating that the deviation observed in Fig. 5 is caused by the size effect. Notably, the particle number in the sc lattice with $4 \times 4 \times 4$ cells is only 64. The plateau values obtained from the $6 \times 6 \times 6$ and $10 \times 10 \times 10$ unit cells correlate well with the fcc and bcc lattices, revealing the indifferent characteristics of the ideal gas state. Consequently, the results for sc presented below are based on $6 \times 6 \times 6$ unit cells unless otherwise specified.

Area distribution correlates closely with the volume distributions. The change in probability distributions of the surface area of VP with increasing p resembles that for volume distribution, and is illustrated in Fig. 7. However, unlike the volume distribution, the mean of the area distribution is not a constant but rather varies with p. Variance increases with p while M_3 remains around zero, matching a broadening, but almost symmetrical Gaussian distribution. The mean area distribution increases with p for bcc and fcc lattices, which have compact original packing and a minimum surface area of individual VP. Any perturbation generates a pair of VP, one larger and one smaller than the original lattice. The net effect is an increase in mean area since the larger VP contributes more than the

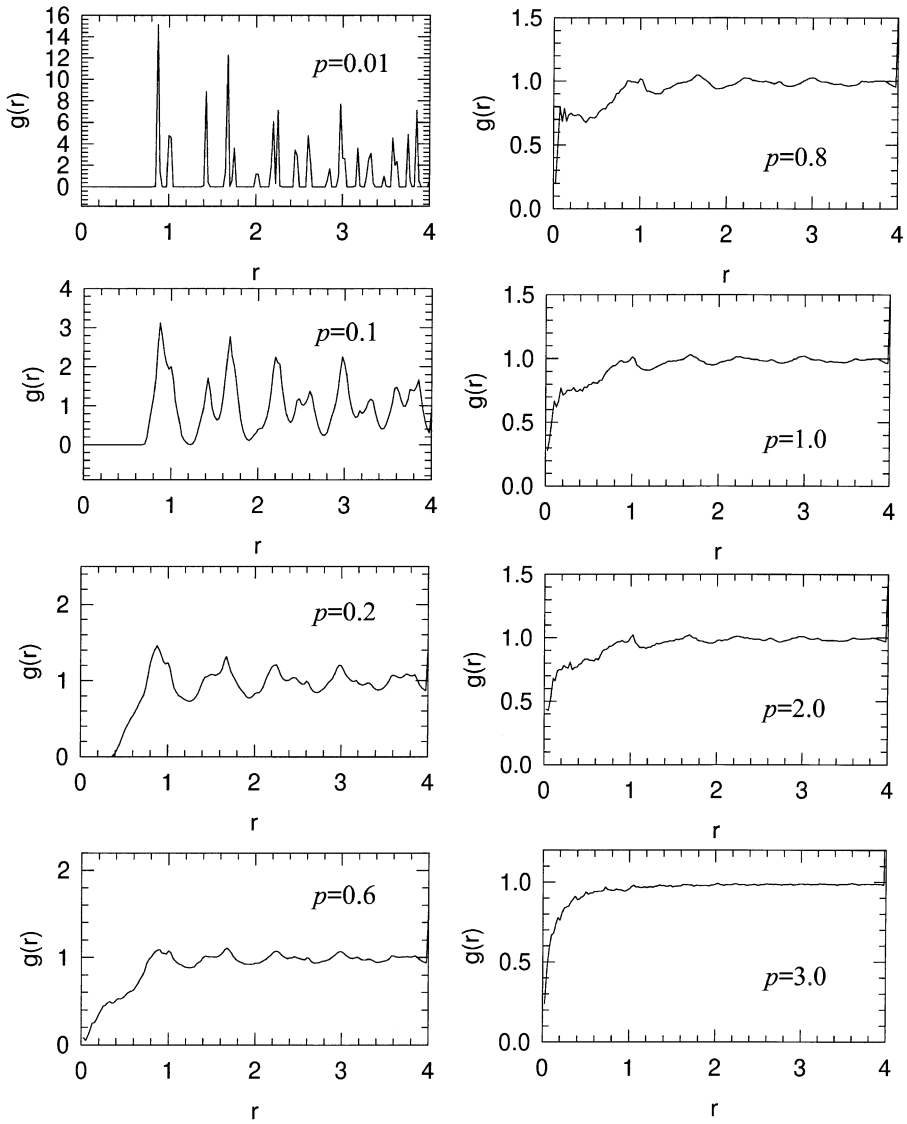

Fig. 3. The RDFs for a bcc lattice subject to perturbation using Scheme 1.

smaller ones. For sc lattices, however, the original packing is loose. Perturbation tends to first "destroy" some surface areas until $p = 0.35$, and then the contribution of random packing arises, causing surface area to increase again.

The distributions for the asphericity parameter resemble those of the volume and area distributions, and Fig. 8 illustrates the mean, variance and M_3 value of the asphericity parameter. When p is small, the means of the asphericity parameter for fcc, bcc and sc are 1.33, 1.35, and 1.91, respectively. These values, together with variance and M_3 values of nearly zero correlate with the original crystal shapes. For a greater p, all distributions converge to that for an ideal gas, which is a skewed normal distribution with mean of 1.96, variance of 0.135, and M_3 of 2–3. Restated, the asphericity parameter of VP for the ideal-gas state ranges mostly between 1.3 and 2.5, and thus covers a wide range of VP shapes.

Between the above two extremes the configurations change. While $p = 0.1$–0.2, where solid/liquid transition occurs, the corresponding variance is essentially zero, reflecting that the shapes of VP in the lattice are mostly the same. For fcc and bcc lattices, η increases from 1.33–1.35 to 1.46 or 1.56, respectively. Consequently, the transition from crystal to liquid configurations yields 9 to 11-face polyhedra to the 12-face polyhedra of the original VP. Again, the shapes of VP for sc differ from those of the other two lattices. When $p = 0.1$–0.2, the variance is still close to zero. However, the shapes of VP for sc change from being simple cubes (1.91, 6-face) into octahedrons (1.65, 8-face). Restated, the "melting" of the sc lattice would reduce rather than increase the η value. Such an observation correlates with the decrease in surface area noted in Fig. 8a. Notably, at $p = 0.3$, the means of the asphericity parameters for the three lattices are close

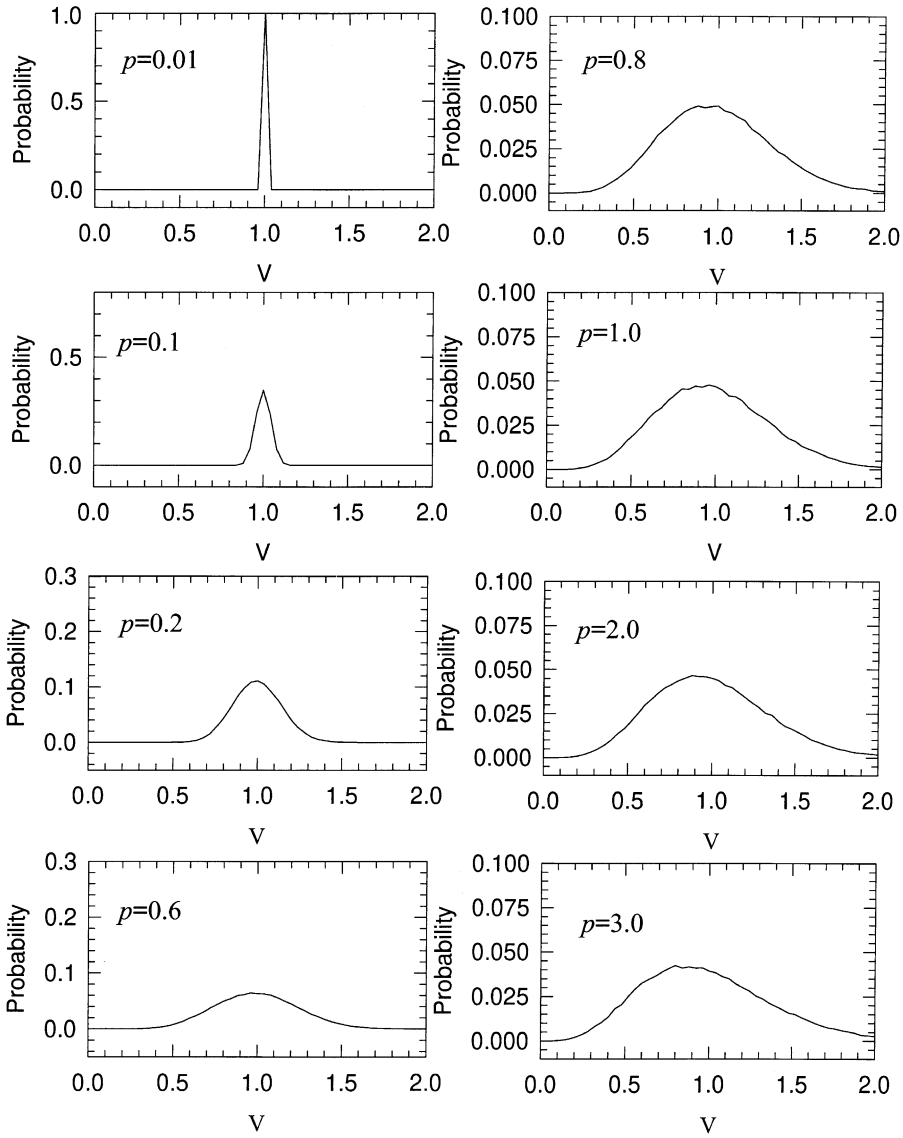

Fig. 4. Volume distributions for bcc lattice perturbed at varying p.

(1.63–1.72). Meanwhile, the corresponding variance also grows. Thus, the transition from crystal to liquid configurations generally transforms the original shapes into polyhedra with 8–11 faces, regardless of its original configurations.

During the transition from the liquid to gas states the shape distribution broadens markedly, as evidenced by the rapid increase in the variance values. The fcc and bcc lattices become completely random at a lower p than the sc lattice. The transition from the liquid to gas configurations thus mainly transforms the polyhedra of 8–11 faces into a wide spectrum of shapes, from those close to close-packing of particles (12-face) to those with a shape that is far away from spherical, like tetrahedron (4-face).

The asphericity distributions for sc at various unit-cells numbers are found to be almost identical, even for the case of $4 \times 4 \times 4$ unit cells. Consequently, η is less sensitive to system size than the volume and the area distributions. From this perspective, the asphericity parameter is thus superior to the volume and area distributions. Furthermore, η provides more structural information than the volume and area distributions [9,11].

Above discussions are deal with equilateral polyhedra. Actually, the distortion or elongation of a polyhedron could yield a higher η value. VP are seldom equilateral, and consequently the η alone is not satisfactory to determine the VP shape. However, except for on tetrahedrons, the effects of VP distortion on η are found to be secondary to the effect of the VP shape itself. For example, for an octahedron, a minor distortion of the shape would only slightly change η, at a value all around 1.65 regardless of the degree of elongation. Therefore, the general discus-

sions on VP shape agree with the idea that the evolution of η should be sufficient if given small corresponding variance. However, no conclusion on the exact shape of VP is possible if the corresponding variance is large.

Fig. 9 illustrates the face-number distributions for fcc, bcc and sc at $p = 0.001$. As Fig. 9 reveals, the face-number of VP for bcc is a single value: 14. However, the face-number distributions for fcc and sc are much greater than for bcc. These observations differ significantly from the asphericity parameter data discussed above. A typical Voronoi polyhedron for sc lattice perturbed at $p = 0.001$ exhibits a cubic shape with six faces (squares) to the naked, and has an asphericity parameter of 1.909. However, such a polyhedron actually has 11 faces: one triangle, four tetragons, two pentagons, three hexagons and one heptagon, recorded as $(F_3,F_4,F_5,F_6,F_7) = (1,4,2,3,1)$. Small cuts at the edges create the non-square faces, which cannot be identified as non-squares by their appearance or by the asphericity parameter. However, the face-number distribution considers all small cuts. Consequently, face-number is inappropriate for judging the gross shapes of VP. However, face-number distribution correlates with the distribution of the nearest neighbor or the coordination number [27], which is essential to determine many effective transport properties in a packed system [28].

Two peaks appear in the face-number distribution for the bcc lattice with a small p, and collapse rapidly as p exceeds 0.1–0.2, corresponding to the solid/liquid transition [8]. No liquid/gas transition could be detected at higher increments of p. Since the face-number distributions for fcc and, especially, for sc, are rather broad at small p, their mean or variance cannot differentiate the configuration change even for the solid/liquid transition. Finney [4] proposed that the appearance of triangles in VP could detect the solid/liquid transition. Finney's proposal was verified herein, since triangles really do appear as transition occurs. However, no universality is apparent when applying this index in applications for configurations other than those investigated herein.

Based on the face-distribution Hsu and Mou [8] proposed that the configurational entropy change contributes to most of the total entropy change to solid melting. From the definition of Boltzmann–Gibbs, the entropy of a distribution is proportional to the logarithm of its variance (σ). For example, when the normal distribution and exponential distribution are defined as follows:

$$\Psi = \frac{1}{\sqrt{2\pi}\,\sigma}\exp\left(-b^2/2\sigma^2\right), \tag{4a}$$

$$\Psi = \exp\left(b/\sqrt{\sigma}\right)/\sqrt{\sigma}, \tag{4b}$$

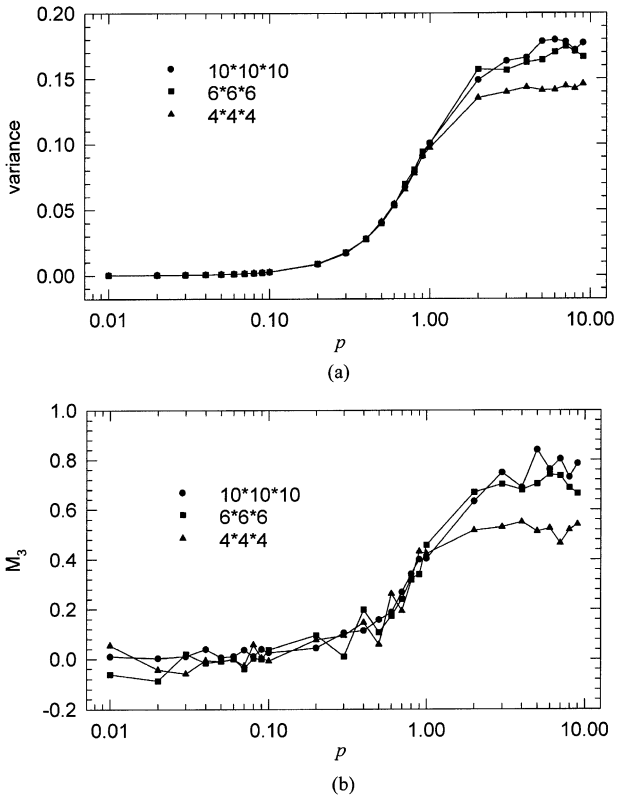

Fig. 6. Variances (a) and M_3 value (b) of the volume distributions with sc lattices of $4\times4\times4$, $6\times6\times6$ and $10\times10\times10$ unit cells. Scheme 1.

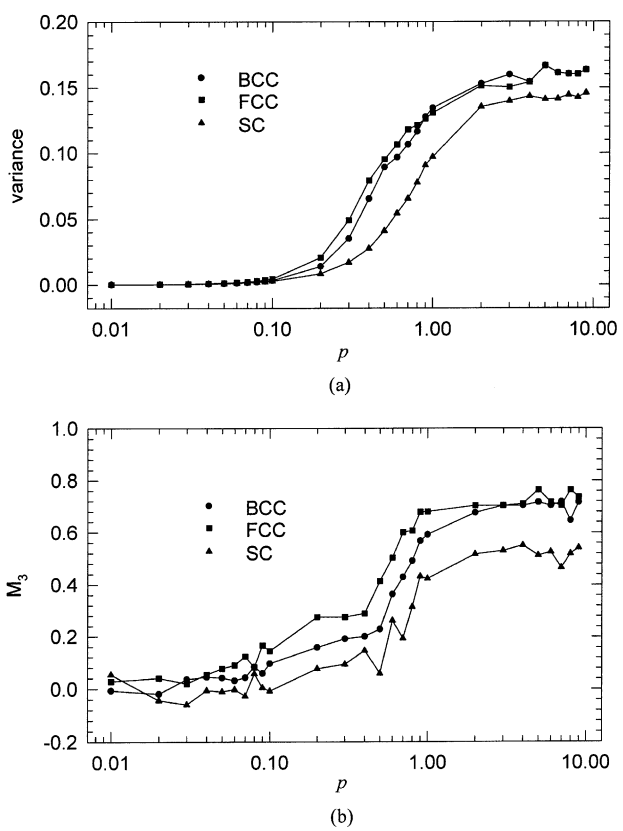

Fig. 5. Variances and M_3 value of the volume distributions in Fig. 4.

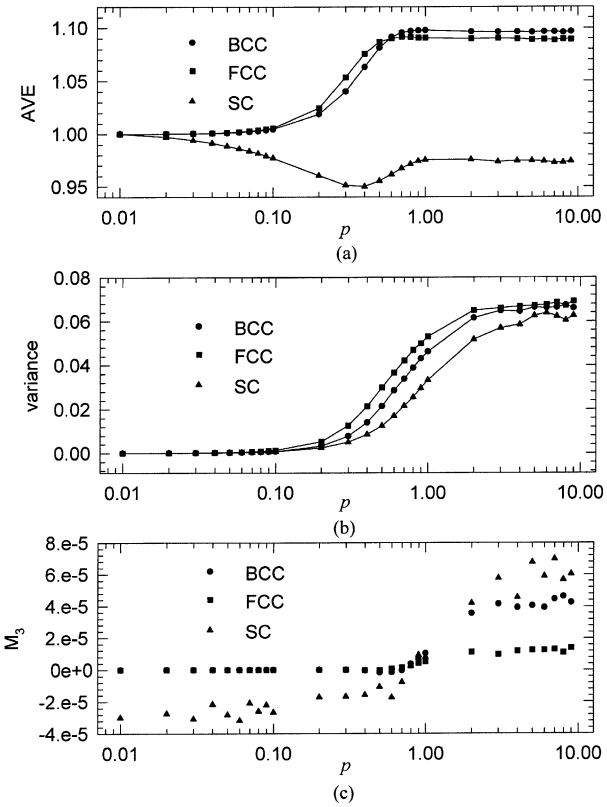

Fig. 7. Surface area distributions at varying p. (a) Mean (b) variance (c) M_3 value.

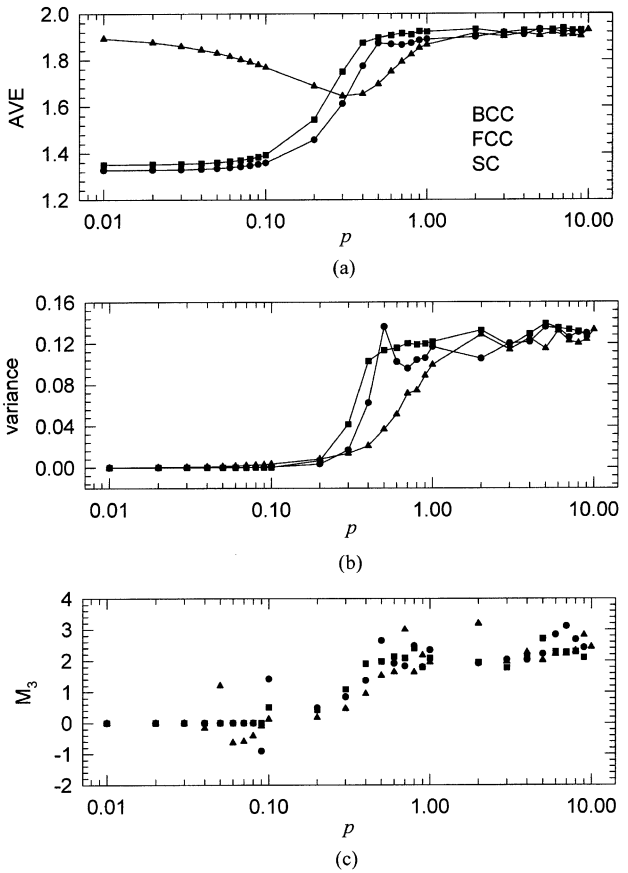

Fig. 8. Asphericity parameter distributions at varying p. (a) Mean (b) variance (c) M_3 value.

then the S_b value could be derived as:

$$S_b = \ln\sqrt{2\pi}\,\sigma + 1/2, \tag{5a}$$

$$S_b = \ln\sigma/2 + 1. \tag{5b}$$

Moreover, with a uniform distribution of Ψ, $S_b = \ln\sigma/2 + \ln 12/2$.

Fig. 10 presents the Boltzmann–Gibbs entropy for the volume distribution displayed in Fig. 4, together with its variance. The figure reveals a linear correlation, inferring that the BG entropy is also proportional to the distribution variance. Consequently, extracting more information from the BG entropy than from the other VP distributions is impossible.

VP or other microstructural descriptors are employed to provide detailed information about the local structure of multi-particle systems. Most authors agree that VP could provide more information than the RDFs. Meanwhile, some investigations conclude that the asphericity parameter is superior to the other VP characteristics for their specific applications. However, the results herein reveal that the applicability of certain VP descriptors depends heavily upon the nature of the system and the intended applications. Since the present study adopted a simulated system with controlled disorderliness, the capability of VP descriptors could be compared continuously.

If analysis were to reveal solid/liquid transition, RDFs are adequate indices. However, VP contain more microstructural information. The asphericity parameter distribution provided information on both the solid/liquid and liquid/gas transitions, while the volume distribution is less sensitive than the asphericity parameter for identifying the solid/liquid transition. Face-number distribution is important in determining the coordination number distribution. However, face-number distribution may mislead the judgment of the overall VP shapes in the systems. Meanwhile, while Boltzmann–Gibbs entropy can estimate the entropy

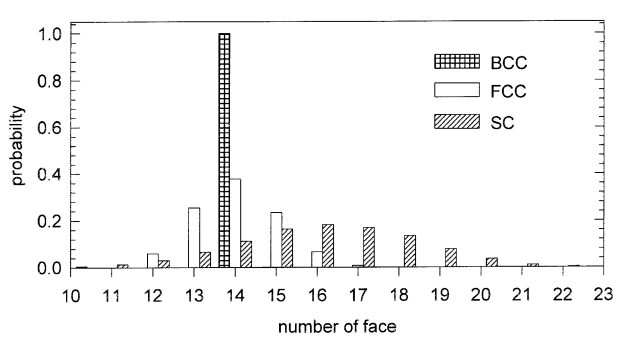

Fig. 9. Face-number distributions for fcc, bcc and sc at $p = 0.001$.

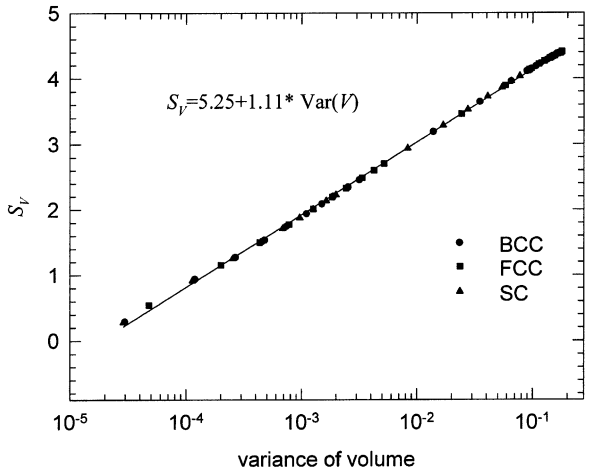

Fig. 10. Entropy S_V versus variance of volume distributions for fcc, bcc and sc.

change during phase transition, its insights into the process are no better than the other VP descriptors. Therefore, when applied, all VP descriptors could describe certain aspects of the microstructure being investigated. Thus, no single VP descriptor is really superior to the others.

4. Conclusions

The Voronoi polyhedra (VP) analysis for describing simulated multi-particle systems with controlled disorderliness has been applied to three lattice systems: a face-centered cubic (fcc) lattice, body-centered cubic (bcc) lattice or a simple cubic (sc) lattice. The position of each particle is then perturbed by three different schemes at a controlled magnitude. The radial distribution function (RDF) differentiates the phase transition between the gas-like, liquid-like, and the solid-like states. The probability distributions for number of faces, area, volume, and asphericity factor are then calculated. The asphericity parameter distribution identified both the solid/liquid and liquid/gas transitions. Meanwhile, the volume distribution is not suitable for identifying the solid/liquid transition. Furthermore, the face-number distribution reflects the coordination number distribution of VP, but might yield erroneous results for the overall VP shape descriptions. The Boltzmann–Gibbs entropy provides no deeper insights into the process than other VP descriptors. Rather, all VP descriptors could clarify certain aspects of the microstructure being investigated.

5. List of symbols

A surface area of VP
b physical quantity of interest
F_i number of i-face
f_i $= \Psi \Delta b$
N step number for perturbations
p degree of disorderliness
Δr step length of perturbation
S_b entropy for property b
S_V entropy for VP volume
V volume of VP

Greek letters

Ψ probability density function of the physical quantity b
η asphericity parameter
σ variance of the distribution

Acknowledgements

The authors appreciate Prof. C.Y. Mou of the Department of Chemistry, National Taiwan University, for providing the VP program.

References

[1] G.F. Voronoi, J. Reine, Angew. Math. 134 (1908) 198.
[2] J.D. Bernal, Proc. R. Soc. London, Ser. A 280 (1964) 299.
[3] J.D. Bernal, J.L. Finney, Discuss. Faraday Soc. 43 (1967) 62.
[4] I.L. Finney, Proc. R. Soc. London, Ser. A 319 (1970) 495.
[5] M.R. Hoare, J. Non-Cryst. Solids 31 (1978) 157.
[6] H.C. Hsu, A. Rahman, J. Chem. Phys. 71 (1979) 4979.
[7] G. Ruocco, M. Sampoli, R. Vallauri, J. Mol. Struct. 250 (1991) 259.
[8] T.J. Hsu, C.Y. Mou, Mol. Phys. 75 (1992) 1329.
[9] J.C.G. Motoro, J.L.F. Abascal, J. Chem. Phys. 97 (1993) 4211.
[10] J.C.G. Motoro, F. Bresme, J.L.F. Abascal, J. Chem. Phys. 101 (1994) 10892.
[11] J.P. Shih, S.Y. Sheu, C.Y. Mou, J. Chem. Phys. 100 (1994) 2202.
[12] M.I. Aoki, K. Tsumuraya, J. Chem. Phys. 104 (1996) 6719.
[13] P. Jund, D. Caprion, R. Jullien, Europhys. Lett. 37 (1997) 547.
[14] A. Baranyai, I. Ruff, J. Chem. Phys. 85 (1986) 365.
[15] A. Goede, R. Preissner, C. Frommel, J. Comput. Chem. 18 (1997) 1113.
[16] J. Bohm, M. Bohm, R.B. Heimann, Cryst. Res. Technol. 31 (1996) 1069.
[17] N.W. Thomas, Acta Crystallogr., Sect. B: Struct. Sci. 52 (1996) 939.
[18] S. Ghosh, Z. Nowak, K. Lee, Acta Mater. 45 (1997) 2215.
[19] S. Moorthy, S. Ghosh, Comput. Methods Appl. Mech. Eng. 151 (1998) 377.
[20] R.E. Eils, K. Bertin, B. Saracoglu, E. Rinke, F. Schrock, Y. Parazza, M. Usson, Z.H.K. Robertnicoud, J.M. Stelzer, T. Chassery, C. Cremer, J. Microsc. 177 (1995) 150.
[21] M. Gerstein, J. Tsai, M. Levitt, J. Mol. Biol. 249 (1995) 955.
[22] J.D. Rogers, R.L. Long, J. Membr. Sci. 134 (1997) 1.
[23] P.L. Spedding, R.M. Spencer, Comput. Chem. Eng. 22 (247) (1998) 247.
[24] D.H. Everett, Discuss. Faraday Soc. 43 (1967) 82.
[25] Y.C. Liao, D.J. Lee, Chem. Eng. Commun. 176 (1999) 77.
[26] M. Tanemura, T. Ogawa, N. Ogita, J. Comput. Phys. 51 (1983) 191.
[27] R. Collins, T. Ogawa, T. Ogawa, Prog. Theor. Phys. 78 (1987) 83.
[28] M. Tassopoulos, D.E. Rosner, AIChE J. 38 (1992) 15.